INTERNATIONAL JOURNAL OF INTEGRATED ENGINEERING
ISSN: 2229-838X e-ISSN: 2600-7916

IJIE

Vol. 17 No. 4 (2025) 114-126
https://publisher.uthm.edu.my/ojs/index.php/ijie

Metal Film-Based Flexible Sensor for Omnidirectional Airflow Measurement

Sukarnur Che Abdullah[1], Mohamad Hadis Azmi[1], Mohammad Azzeim Mat Jusoh[1]*, Mohamad Dzulhelmy Amari[1]

[1] *School of Mechanical Engineering, College of Engineering, Universiti Teknologi MARA, 40450, Shah Alam, Selangor, MALAYSIA*

*Corresponding Author: m_azzeim@uitm.edu.my
DOI: https://doi.org/10.30880/ijie.2025.17.04.010

Article Info

Received: 8 March 2025
Accepted: 29 August 2025
Available online: 19 September 2025

Keywords

Sensor, airflow model, flexible, velostat, thermoplastic elastomer

Abstract

The previous study on airflow sensors were fabricated using a flap device printed using polylactic acid (PLA) plastic, which had high stiffness, preventing the sensor from bending and returning to its original shape. The used aluminium (Al) strips exhibited relatively higher resistance values compared to copper (Cu), resulting in inconsistent resistance readings at various angles of bending measurement. This paper presents a new development of an enhanced metal film-based flexible sensor for application on omnidirectional 360-degree airflow measurement. The sensor was fabricated using copper film and velostat, a material made of polymeric foil (polyolefins) infused with carbon black to make it electrically conductive. The flapping device was modelled in SolidWorks (3D CAD) and printed using TPE 83A (Thermoplastic Elastomer) filament on a 3D printing machine. An Arduino Mega was used as a controller, data collector, and for evaluating the results. The copper film and TPE 83A material demonstrated significant potential in developing a new flexible sensor for achieving high-accuracy airflow measurement in omnidirectional.

1. Introduction

The demand for advanced sensor technologies has intensified due to their critical role in modern applications ranging from robotics and wearable health systems to environmental and industrial monitoring. Among various types of sensors, flexible and airflow sensors have garnered significant attention owing to their high sensitivity, stretchability, mechanical compliance, and rapid response characteristics [1~3]. These sensors are particularly advantageous for applications that involve dynamic mechanical deformation, such as human motion tracking and robotic manipulation, where rigid sensors fall short [4~6].

Recent developments in nanomaterials and functional composites have further enhanced sensor performance. Conductive nanomaterials such as silver nanowires, graphene, and carbon black provide superior electrical properties while maintaining mechanical flexibility [7~10]. Their integration into flexible substrates like polyimide, velostat, or thermoplastic elastomers enables the fabrication of sensors with high signal resolution and robustness under repeated bending or stretching cycles.

Fabrication techniques such as hybrid 3D printing and microstructure-guided assembly have been employed to engineer sensor architectures with precise geometrical control and tuneable mechanical properties [11~14]. These techniques allow the realization of airflow sensors capable of detecting low and multidirectional airflow velocities, critical for applications in HVAC systems, biomedical diagnostics, and aerospace navigation [15~17]. For instance, iontronic sensors and alternating current electroluminescent devices exhibit high responsiveness under complex deformation conditions, thus making them suitable for intelligent sensing environments [18~20].

This is an open access article under the CC BY-NC-SA 4.0 license.

Multilayer flexible sensors using ferroelectric or triboelectric layers have demonstrated improved signal linearity and stability under fluctuating loads, while serpentine-shaped conductors bonded to elastomers offer superior stretchability with minimal mechanical fatigue [21~25]. Furthermore, sensor calibration and structural optimization are essential for ensuring measurement reliability, especially in macrofluidic systems exposed to turbulent flow or multi-axis displacement [26~28].

This paper builds upon these foundational advancements by proposing a metal film-based flexible airflow sensor that employs a copper-velostat laminate structure integrated with a thermoplastic elastomer flap. The novel configuration is designed to measure omnidirectional airflow effectively. The design is further validated using a series of calibration experiments inspired by prior work in macrofluidic airflow modelling and flap-based airflow detection [27, 29~32]. This study aims to demonstrate that integrating low-resistance copper foil and elastic flap structures can yield highly responsive and cost-effective sensors for next-generation omnidirectional airflow sensing platforms.

This research explores these potentials by fabricating a new design of a flexible sensor that can work as an element in an airflow measurement device. The main objectives are to model an enhanced version of a flexible sensor using copper films. By using Arduino as a controller, this project will evaluate the developed flexible sensor under different flap widths from 1.0mm to 5mm and analyze the resistance readings based on different widths of copper foil on flap sensors.

2. Methodology

Fig. 1 shows the prototype of the enhanced metal film-based flexible sensor for measuring omnidirectional airflow has been conducted in stages to achieve this research's objectives. The methodology that can be adapted to this research is listed below:

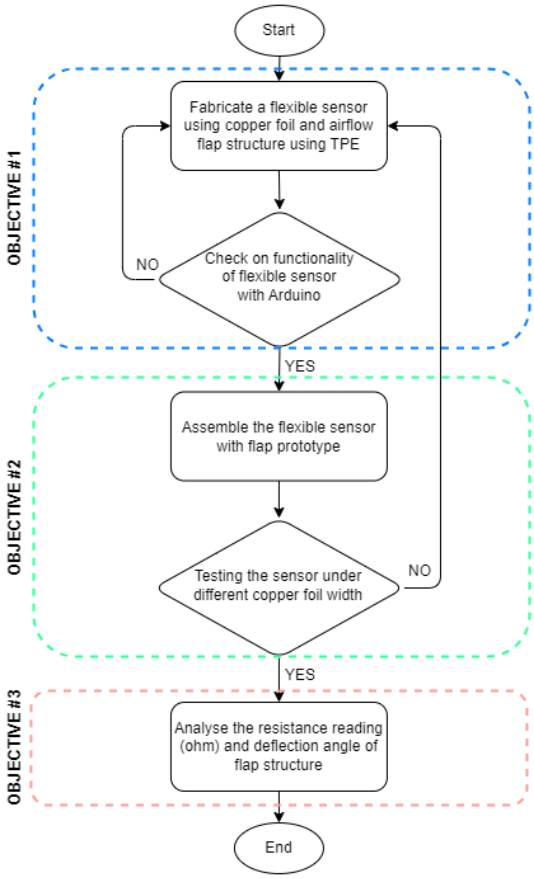

Fig. 1 *Flow chart of the methodology*

Stage 1: Identify and compare the model from previous research with the latest technologies.
Stage 2: Generate a new prototype model for flexible sensors and airflow flap structure.
Stage 3: Testing and calibrating the sensor.
Stage 4: Evaluate the result and analyze the system.

Int. Journal of Integrated Engineering Vol. 17 No. 4 (2025) p. 114-126

2.1 Material Selection

Material selection in this study will consist of two different components. For the first component, the model of a flexible sensor will be fabricated using metal-film-based, velostat, and plastic substrate. Based on past research, the suitable material to fabricate a flexible sensor is by using copper (Cu) foil because it contains a low resistivity value and, also exhibits a dependable result in terms of the flex sensor's working principle, in contrast to aluminium (Al), which was unable to satisfy the sensor's requirements [33]. The flap structure is the second component that will be fabricated in this study. The flap structure must be made of elastic material, high flexibility, and low stiffness so that the flap can return to its original form after bending. ABS plastic is not relevant due to less elasticity and flexibility, making the flap hard to bend [34]. The flexible airflow sensor was developed using a copper-velostat laminate structure mounted onto a 3D-printed TPE 83A flap. Copper was selected due to its low resistivity and stable performance under cyclic bending conditions [27, 30~33], while velostat provides pressure-sensitive resistance variability. TPE 83A was chosen for its flexibility and high fatigue resistance, allowing the flap to return to its original form post-deflection [12, 17].

2.2 Models of Flexible Sensor

In this stage, the details of the flexible sensor models will be explained. The basic flexible sensor concept is as shown below: the velostat is placed between two copper films, and the plastic substrate undergoes a laminating process to hold all the components together as Fig. 2.

Fig. 3(a) shows the full dimension of the flexible sensor. Its overall dimensions are 50mm x 10mm. The model in Fig. 3(b) is after the copper films, velostat, and plastic substrate have been laminating together and forming a low-cost flexible sensor. The grid on the background scale on one box is 5mm.

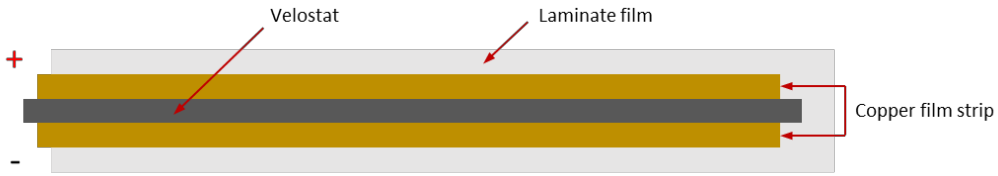

Fig. 2 *The flexible sensor layout*

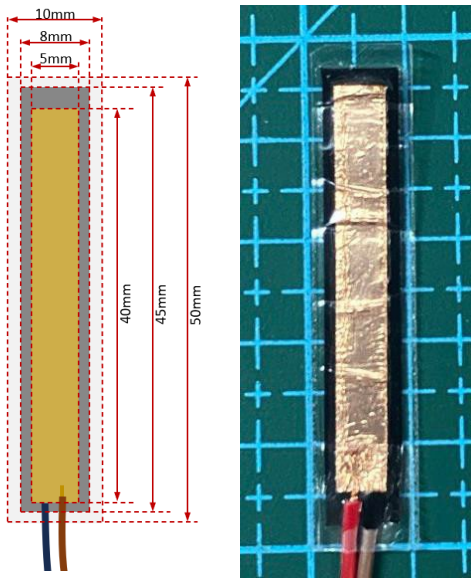

(a) **(b)**

Fig. 3 *(a) Dimension of flexible sensor; (b) Model of flexible sensor*

Each wire was attached to the copper film side, ensuring there's no contact with one another, with velostat serving as the resistive material. The copper films were tailored into three different widths: 1.0mm, 3mm, and 5mm as shown in Fig. 4. The resistance values of these flexible sensors will be measured and analysed in the following chapter.

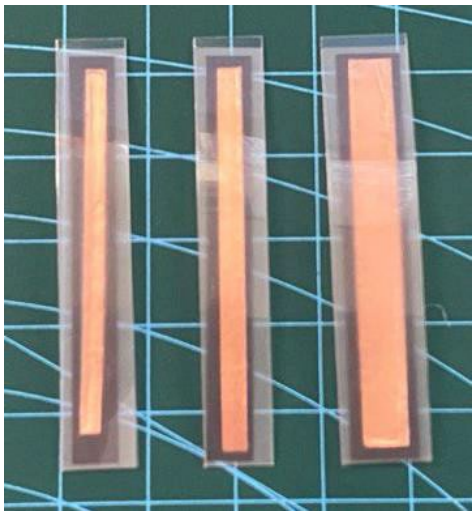

Fig. 4 *Sample of 1.0mm, 3mm, and 5mm copper film on flexible sensor*

2.3 Models of Airflow Sensor

The airflow sensor consists of two main parts: the airflow sensor case and the flap structure. Both components were fabricated using a 3D printing machine and different filaments. The PLA-F filament was applied to the airflow sensor case, as the case needs to be hard and sturdy to withstand the fluid flow of high air velocity. Fig. 5 shows the drawing of the airflow sensor assembly.

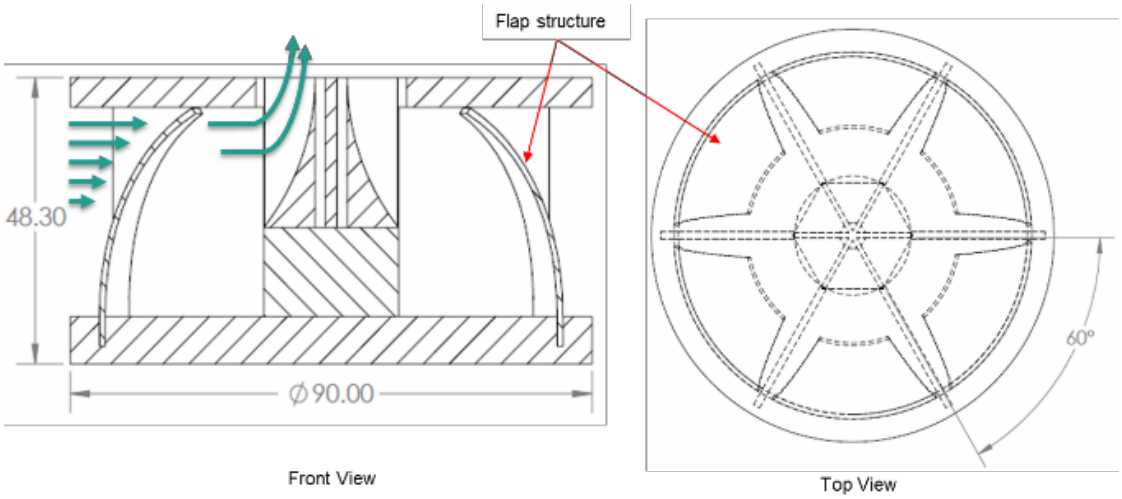

Fig. 5 *Drawing of the airflow sensor assembly*

The dimensions of the flap structure assembly with flexible sensors are shown in the Fig. 6. The material Thermoplastic Elastomer (TPE) 83A shore hardness has been applied on this structure as its properties of flexibility.

Int. Journal of Integrated Engineering Vol. 17 No. 4 (2025) p. 114-126

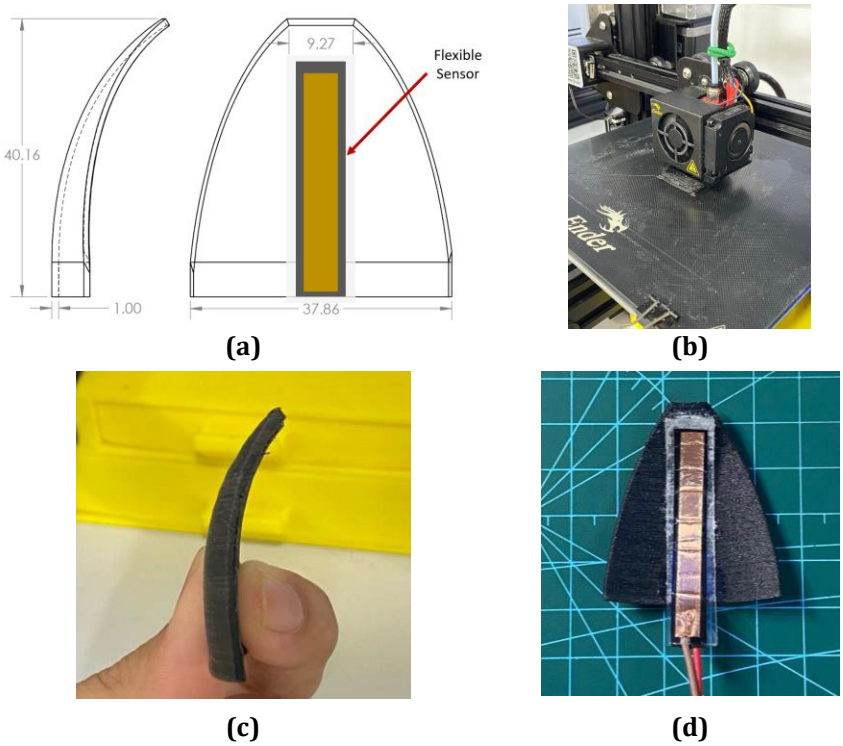

Fig. 6 *(a) Drawing of the flap structure; (b) Flap structure printing; (c) The flap structure model; (d) The assembly of the flap structure and flexible sensor*

2.4 Calibration Using Data Acquisition Tool

Real-time data collection and analysis from a range of sensors is possible with the help of a data acquisition tool called SensorDAQ, as shown in Fig. 7(a). Sensor data collection and processing is common use in research institutions, educational settings, and engineering projects. SensorDAQ is a versatile platform that can be connected to a wide range of sensors, including voltage and current sensors, making it suitable for a wide range of experimental settings. An energy sensor shown in Fig. 7(b) is linked to SensorDAQ; a device specifically designed to detect electrical parameters such as voltage, current, power, and energy consumption. These sensors are necessary for monitoring and assessing flexible sensor performance because they allow precise measurements of the electrical characteristics of systems and individual parts.

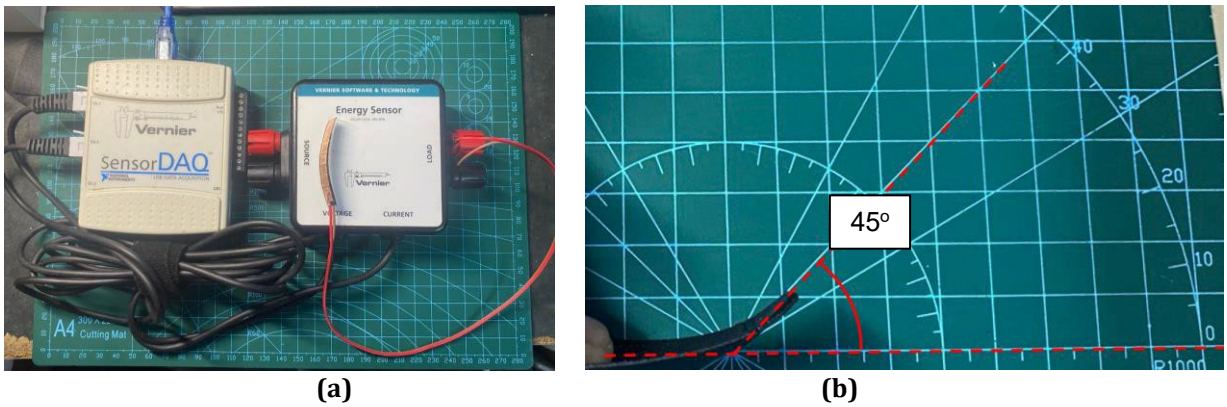

Fig. 7 *(a) SensorDAQ connected with energy sensor; (b) Flap structure angle at a static state*

The energy sensor continuously measures the voltage, records the flexible sensor current flow, and transmits the information to SensorDAQ. The voltage and current fluctuate in response to changes in the flexible sensor, which can be monitored through the computer's Logger Pro software. The resistance value can be obtained as Eq. (1):

$$R = V/I \quad (1)$$

The equation can be inserted into the software, and the data collecting process was performed three times for each copper foil's width (1.0mm, 3mm, 5mm), starting with 45° of angle bend until 90° (maximum bend) flexible sensor. Fig. 8 shows the data obtained on Logger Pro software.

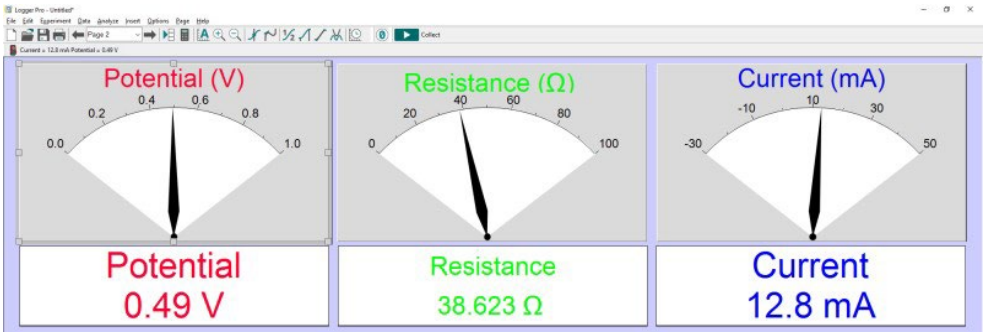

Fig. 8 *Logger pro software interface*

2.5 Arduino Mega Programming Setup

A microcontroller board built around the ATmega2560 chip using Arduino Mega. It is a member of the Arduino development board family and is built to provide more memory, processing power, and input/output (I/O) pins than the Arduino Uno and other standard Arduino boards. The Arduino Mega has been used because it has 16 analog input pins, unlike Arduino Uno, which only has 6 analog input pins, as shown in Table 1. A flexible sensor requires an analog input pin to gain data, and for this sensor, six analog input pins were used for six flexible sensors, which are for one flexible on each flap structure on this model. Arduino Uno only has six analog input pins, but pins A4 and A5 limit to connect serial data line (SDA) and a serial clock line (SCL) that are used in the integrated-circuit protocol (I2C) such as LCD displays.

Table 1 *The Arduino UNO and MEGA specifi catio ns [10]*

ARDUINO	UNO	MEGA
Microcontroller	ATmega328	ATmega2560
Digital I/O Pins	14	54
Operating Voltage	5V	5V
Analg Input Pins	6	16
Flash Memory	32 KB	256 KB
SRAM	2 KB	8 KB
EEPROM	1 KB	4 KB
Clock Speed	16 MHz	16 MHz

The system integrations on this airflow sensor model as shown in Fig. 9(a); the six flexible sensors were connected on analog input pins A0, A1, A2, A3, A4, and A5 and assigned as flex sensor values S1, S2, S3, S4, S5, and S6 on the Arduino system. LCD I2C 4 x 20 was then connected to the SDA and SCL pins to fetch the data gain on bending changes. Fig. 9(b) shows the final airflow sensor model connected with the Arduino system, and the value shown on the LCD was the value of each flexible sensor on the flap structure. The Arduino Mega 2560 microcontroller was implemented for data acquisition, offering 16 analog input pins suitable for multi-sensor deployment. This configuration supports real-time data display using a 20 x 4 LCD via I2C communication [8, 28, 35]. The system was programmed to acquire, convert, and display resistance values from each flap sensor.

Int. Journal of Integrated Engineering Vol. 17 No. 4 (2025) p. 114-126

The adopted methodology aligns with best practices in flexible sensor development, incorporating modular fabrication, stretchable materials, and robust calibration strategies for effective multidirectional airflow detection [21, 23~25].

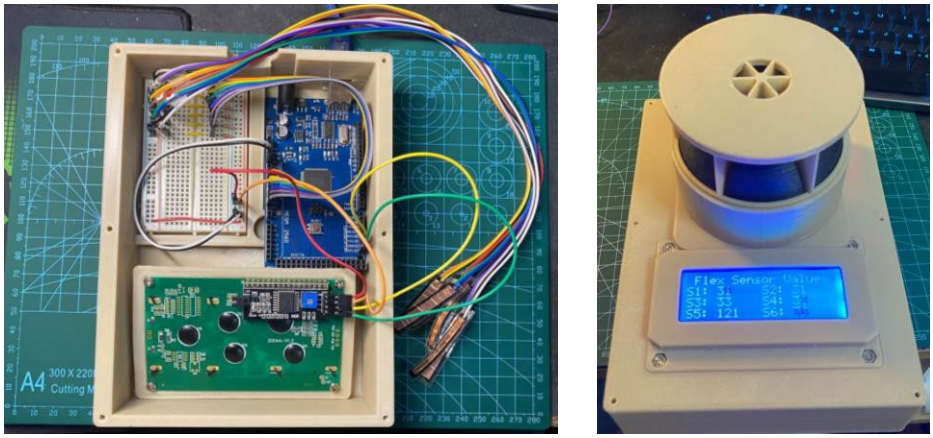

(a) **(b)**

Fig. 9 *(a) The Arduino mega programming setup; (b) The airflow sensor model integrates with Arduino mega*

2.6 Flexible Sensor Selection

As shown in Fig. 10 below, the flexible sensor undergoes bending testing, and the resistance value and Arduino value were recorded for each angle interval from 45° to 90° bend angle.

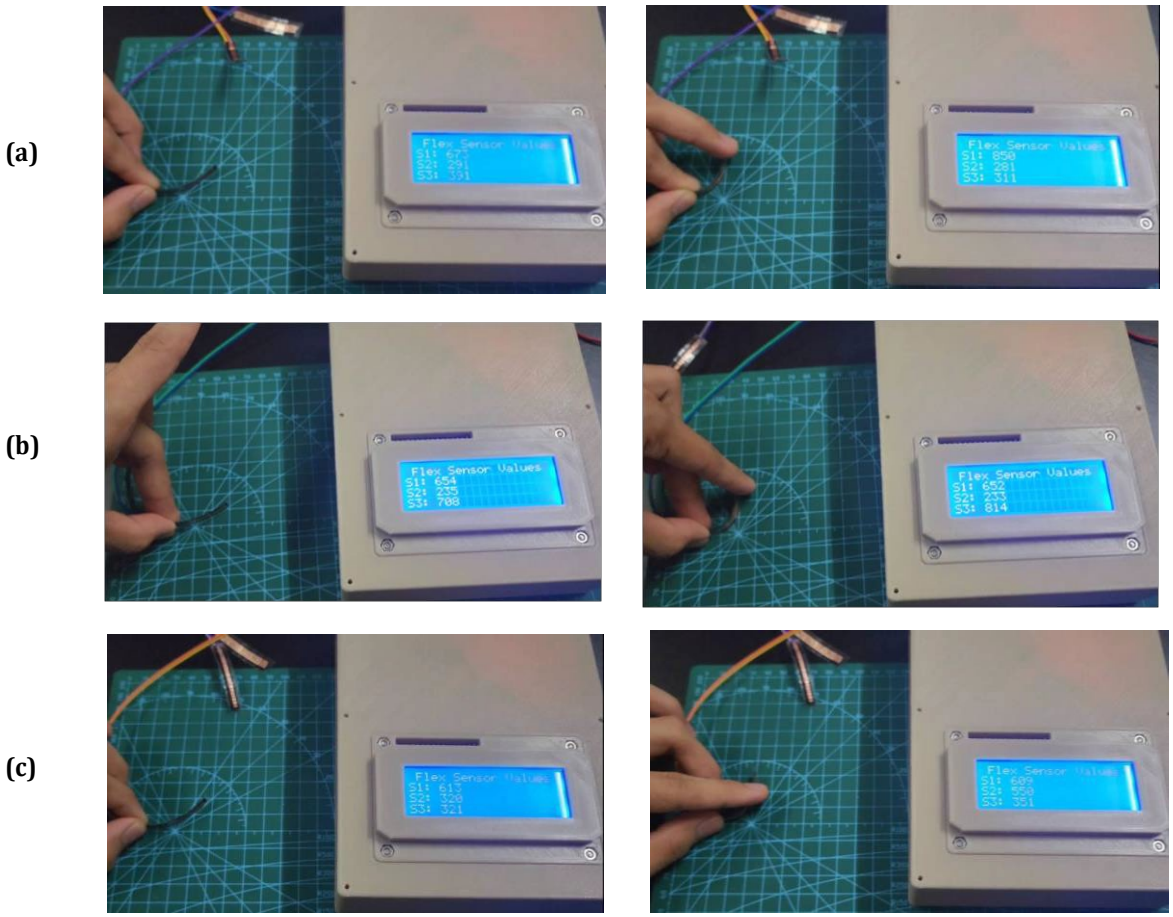

(a)

(b)

(c)

Fig. 10 *(a) 1.0mm width flexible sensor bend testing; (b) 3mm width flexible sensor bend testing; (c) 5mm width flexible sensor bend testing*

3. Results and Discussion

3.1 Resistance on Each Width Flexible Sensor

The data on a flexible sensor using copper foil with a width of 1.0mm as demonstrates in Fig. 11(a), shows a steady rise in resistance with increasing bend angle. Resistance values start at 8.34 ohms and increased up to 8.85 ohms at 45° angle and then increased progressively to 51.60 and 52.74 ohms at 90° angle. Up to 60° angle, the increase in resistance is rather gradual; after that, it becomes more noticeable. Significant divergence in resistance values is observed starting at 66° angle, which may indicate non-uniform stress distribution or material irregularities. This behaviour suggests that although the bending of copper foil with a width of 1.0mm increases resistance consistently, at larger bend angles, the consistency of the material properties may be questioned.

By contrast, the initial resistance values at 45° angle are significantly higher for the 3mm width copper foil as shown in Fig. 11(b), ranging from 8.67 to 9.23 ohms. At 90°, the resistance rises to 42.80 to 45.45 ohms, increasing gradually with the bend angle. When compared to the 1.0mm foil, the 3mm foil exhibits a smoother and more constant increase in resistance, showing less variance even at greater angles. This homogeneity implies that the 3mm foil controls mechanical stress better, which makes it a more dependable choice in situations where consistent resistance variations are essential.

With initial resistance values ranging from 10.63 to 20.41 ohms at 45°, the copper foil with a 5mm width displays the highest values as Fig. 11(c). It also shows a faster increase in resistance with bend angles. The resistance ranges from 62.72 to 95.00 ohms at 90°. Not only does the 5mm foil exhibit a greater resistance rise, but it also exhibits greater variance and larger leaps at higher angles. This implies that there is greater mechanical strain and difficulty in sustaining uniform conductivity in the 5mm foil under bending force. There is a crucial point where the mechanical strain becomes excessive or where the material properties may change significantly, as indicated by the notable increase in resistance between 84° and 90° angle.

By comparing the three foil widths, it was obvious that the behaviour was different when bent. The increase in resistance was more gradually and predictably in the 1.0mm and 3mm widths, but more variable increases and consistently in the 5mm width. While the 3mm width maintains a smoother and more consistent increase over the whole range, the 1.0mm width shows more uniform resistance increases at first but diverges at higher angles. The 5mm width shows more significant difficulties in controlling mechanical stress, even though the resistance is initially higher. This is probably because there is a greater surface area under strain. For this application, the 5mm width is more suitable where higher resistance and great variables are needed to measure the airflow measurement.

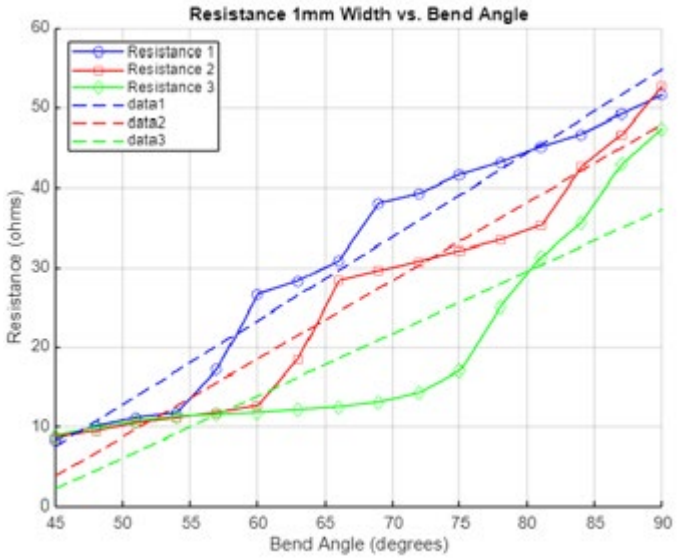

(a)

Int. Journal of Integrated Engineering Vol. 17 No. 4 (2025) p. 114-126

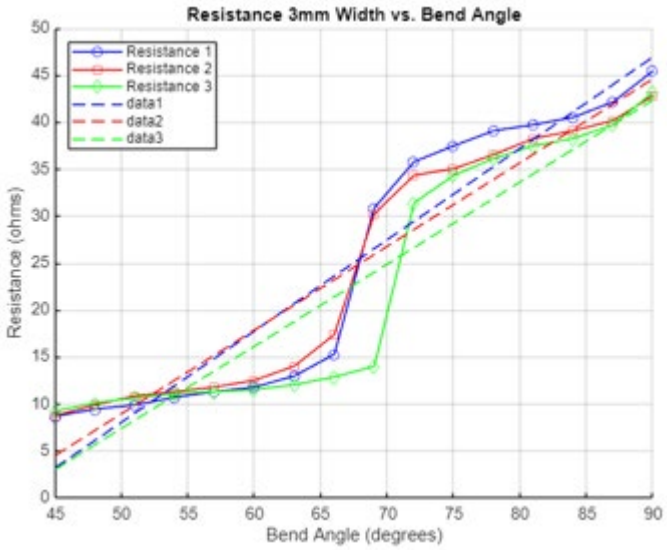

(b)

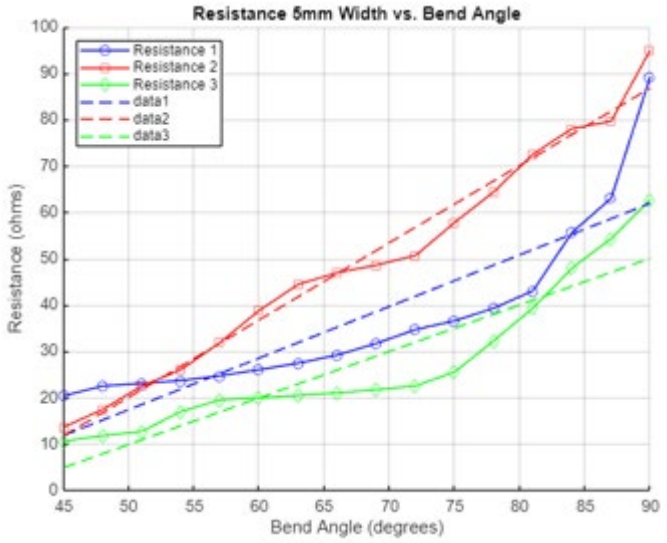

(c)

Fig. 11 *(a) Graph of resistance 1mm width vs. bend angle; (b) graph of resistance 3mm width vs. bend angle; and (c) graph of resistance 5mm vs. bend angle*

3.2 Average resistance

Table 2 shows the average resistance of the copper foil with a width of 1.0mm rises steadily as the bend angle increases. It increases gradually to 50.59 ohms during 90° angle, to 8.62 ohms during 45° angle. The trend is steady and smooth, with noticeable increases, particularly at 57° angle, when the average resistance increases to 17.02 ohms at 60° angle from 13.50 ohms. This behaviour suggests that the 1.0mm foil performs well in situations where fine control over resistance changes with bending is required, as it retains a rather predictable increase in resistance.

The average resistance of the 3mm wide copper foil increases with bending as well, although the pattern is somewhat different from that of the 1.0mm foil. The average resistance begins at 8.88 ohms at 45° angle, which is higher than the 1.0mm foil. The resistance increases gradually up to 60° (11.93 ohms), but at 63° angle it becomes more noticeable. At higher angles, the resistance leaps significantly, reaching at 43.80 ohms at 90° angle. The rise is somewhat gradual but exhibits more noticeable steps beyond 66° angle, indicating that although the 3mm foil effectively handles stress, it starts to feel the effects of greater strain at greater bend angles.

When compared to the narrower foils, the 5mm width copper foil exhibits a significantly higher initial resistance, beginning at 14.90 ohms at 45° angle. The bending causes the resistance to rise quickly; during 48° angle around 17.27 ohms, and at 90° angle, it can reach up to 82.33 ohms. The data in Fig. 12 shows a significant

increase, which is apparent from 60° angle (28.29 ohms) onward. The steep increase and high resistance values indicate that bending has a greater influence on the 5mm foil, resulting in huge variations in resistance due to mechanical stress and strain. So, this width is suitable for applications requiring significant resistance changes with bending, where mechanical design can accommodate high strain and stress impacts. Comparative resistance analysis across different copper widths reveals a trend consistent with stretchable sensing literature [10, 20]. The results align with simulations and calibration approaches reported in recent airflow sensor studies [14, 26~28]. For example, the 5 mm copper foil shows high sensitivity at larger bend angles, confirming trends observed in macrofluidic airflow flap verification [32]. Additionally, the smooth resistance transitions seen in 3 mm width foils correspond to earlier findings where optimized sensor geometries were used to maintain linearity in output data [29, 30].

Table 2 *The average resistance of difference width on copper foil and bend angle*

Bend Angle (°)	Avg Res 1 mm (Ω)	Avg Res 3 mm (Ω)	Avg Res 5 mm (Ω)
45	8.62	8.88	14.90
48	9.80	9.79	17.27
51	10.76	10.45	19.46
54	11.40	11.01	22.26
57	13.50	11.45	25.39
60	17.02	11.93	28.29
63	19.65	13.00	30.81
66	23.88	15.16	32.41
69	26.91	25.00	34.03
72	28.12	33.82	35.98
75	30.23	35.60	40.00
78	33.90	37.23	45.35
81	37.21	38.46	51.63
84	41.64	39.27	60.54
87	46.28	40.66	65.66
90	50.59	43.80	82.33

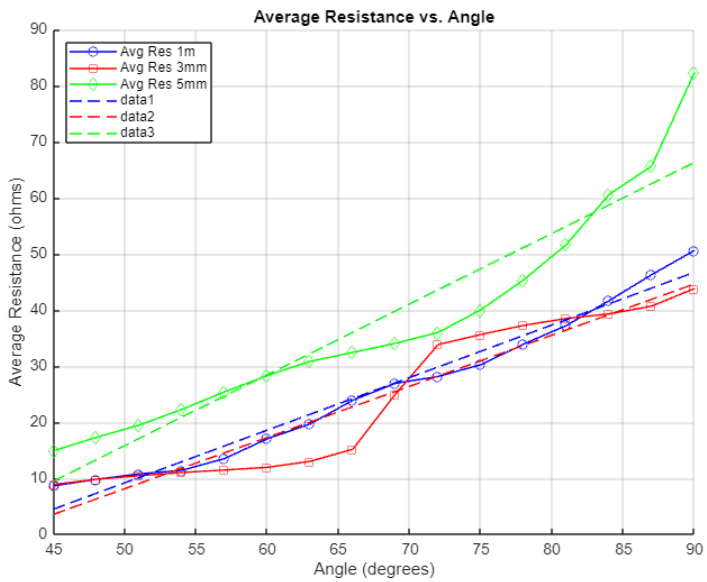

Fig. 12 *Graph of average resistance vs. bend angle*

4. Conclusion

This study presents the development of an enhanced metal film-based flexible sensor for omnidirectional airflow measurement. The methodology of Stage 1 is the model from previous research that has been identified and compared with the latest technologies. This study builds on recent advances in flexible sensor technology [2, 3, 24, 36] and validates its proposed design against prior macrofluidic calibration models [27, 28, 31]. The copper-velostat laminate sensor with a TPE flap demonstrates strong potential as a compact, low-cost, omnidirectional airflow measurement system for emerging applications in robotics, HVAC, and biomedical sensing. This fundamental stage made it possible to create a better sensor prototype. The sensor's performance was validated by extensive testing and calibration, guaranteeing its accuracy and consistency under varied settings. The outcomes of these tests provide comprehensive insights into the behaviour of the sensor, namely the resistance variations that occur when copper foils of various widths 1.0mm, 3mm, and 5mm was bent. The resistance of the 1.0mm wide copper foil increased steadily as the bend angle increased, making it appropriate for applications needing precise control over resistance variations, even if it varied significantly at higher bend angles. The copper foil with a width of 3mm exhibited a more gradual and even increase in resistance, suggesting that mechanical stress was better managed. This makes it a dependable option for applications that require consistent resistance fluctuations.

To improve the sensor's capacity to measure airflow more precisely and consistently, a new prototype model with an innovative airflow flap shape was created. The flexible sensor can be integrated well with the TPE 83A shore hardness material of the flap structure to measure the fluid of airflow just as expected results. The airflow sensor model can measure the airflow from an omnidirectional (360° direction). Overall, the 5mm copper foil is the most suitable for use on flexible sensors as an airflow sensor because of its capability to read great variables of resistance to get more accurate results.

Acknowledgement

Appreciation to College Engineering, Universiti Technologi MARA (UiTM) for their assistance in providing the tools and infrastructure needed for this work.

Conflict of Interest

Authors declare that there is no conflict of interests regarding the publication of the paper.

Author Contribution

The authors confirm contribution to the paper as follows: ***study conception and design:*** *Mohammad Hadis Azmi, Sukarnur Che Abdullah;* ***data collection:*** *Mohammad Hadis Azmi;* ***analysis and interpretation of results:*** *Mohammad Hadis Azmi & Sukarnur Che Abdullah;* ***draft manuscript preparation:*** *Mohammad Hadis Azmi, Sukarnur Che Abdullah, Mohammad Azzeim Mat Jusoh, Mohamad Dzulhelmy Amari. All authors reviewed the results and approved the final version of the manuscript.*

References

[1] Maharjan, P., Bhatta, T., Cho, H., & Park, J. Y. (2020). A highly sensitive self-powered flex sensor for prosthetic arm and interpreting gesticulation. In 2020 IEEE 33rd International Conference on Micro Electro Mechanical Systems, 665-668. https://doi.org/10.1109/MEMS46641.2020.9056118

[2] Pang, C., et al. (2012). A flexible and highly sensitive strain-gauge sensor using reversible interlocking of nanofibres. Nature Materials, 11(9), 795-801. https://doi.org/10.1038/nmat3380

[3] Amjadi, M., et al. (2016). Stretchable, skin-mountable, and wearable strain sensors and their potential applications: A review. Advanced Functional Materials, 26(11), 1678-1698. https://doi.org/10.1002/adfm.201504755

[4] Yao, S., & Zhu, Y. (2014). Wearable multifunctional sensors using printed stretchable conductors made of silver nanowires. Nanoscale, 6(4), 2345-2352. https://doi.org/10.1039/c3nr05496a

[5] Kim, J., et al. (2019). Wearable biosensors for healthcare monitoring. Nature Biotechnology, 37(4), 389-406. https://doi.org/10.1038/s41587-019-0045-y

[6] Zhao, X., & Zhu, Y. (2017). Stretchable, wearable sensors for motion detection and healthcare monitoring. Materials Horizons, 4(3), 379-399. https://doi.org/10.1039/C6MH00632B

[7] Song, T. B., et al. (2015). Highly robust silver nanowire network for transparent electrode. ACS Applied Materials & Interfaces, 7(44), 24601-24607. https://doi.org/10.1021/acsami.5b06540

[8] Li, H., Ding, G., & Yang, Z. (2019). A high sensitive flexible pressure sensor designed by silver nanowires embedded in polyimide (AgNW-PI). Micromachines, 10(3), 206. https://doi.org/10.3390/mi10030206

[9] Rajala, S., & Lekkala, J. (2012). Film-type sensor materials PVDF and EMFi in measurement of cardiorespiratory signals—A review. IEEE Sensors Journal, 12(3), 439-446. https://doi.org/10.1109/JSEN.2010.2094196

[10] Nie, B., et al. (2018). Flexible and transparent strain sensors with embedded microstructures. Advanced Functional Materials, 28(29), 1801279. https://doi.org/10.1002/adfm.201801279

[11] Valentine, A. D., et al. (2017). Hybrid 3D printing of soft electronics. Advanced Materials, 29(40), 1703817. https://doi.org/10.1002/adma.201703817

[12] Fateri, M., et al. (2022). Impact of 3D printing technique and TPE material on the endurance of pneumatic linear peristaltic actuators. Micromachines, 13(3), 392. https://doi.org/10.3390/mi13030392

[13] Castiglioni, S., et al. (2021). Fully printed wearable biosensors for real-time sweat analysis. npj Flexible Electronics, 5(1), 1-8. https://doi.org/10.1038/s41528-021-00123-6

[14] Bendong, T., et al. (2022). 3D-printed microstructure-enhanced flexible sensors for improved airflow detection. Sensors and Actuators A: Physical, 339, 113577. https://doi.org/10.1016/j.sna.2022.113577

[15] Huang, L., et al. (2023). Ultrasensitive, fast-responsive, directional airflow sensing by bioinspired suspended graphene fibers. Nano Letters, 23(2), 597-605. https://doi.org/10.1021/acs.nanolett.2c04228

[16] Li, G., Liu, D., & Yao, L. (2020). A review of flexible and stretchable electronics for monitoring human health. Journal of Materials Chemistry B, 8(19), 4117-4131. https://doi.org/10.1039/d0tb00198g

[17] Xu, L., et al. (2019). Flexible and stretchable sensing systems for wearable electronics. Journal of Materials Chemistry C, 7(47), 15175-15195. https://doi.org/10.1039/C9TC04712F

[18] Wang, J., et al. (2015). Highly stretchable and self-deformable alternating current electroluminescent devices. Advanced Materials, 27(18), 2876-2882. https://doi.org/10.1002/adma.201405486

[19] Araromi, O. A., et al. (2015). Ultra-sensitive and soft capacitive pressure sensors using a composite elastomeric dielectric layer. Nature Communications, 6(1), 1-10. https://doi.org/10.1038/ncomms7635

[20] Wu, Y., et al. (2018). Highly sensitive and wearable iontronic pressure sensors based on gradient PVDF ferroelectric layers. Advanced Functional Materials, 28(22), 1801004. https://doi.org/10.1002/adfm.201801004

[21] Kim, J. H., Oh, J. Y., & Park, J. U. (2021). Stretchable sensors for wearable electronics. Advanced Materials Technologies, 6(7), 2001173. https://doi.org/10.1002/admt.202001173

[22] Maheshwari, V., & Saraf, R. F. (2006). High-resolution thin-film device to sense texture by touch. Science, 312(5779), 1501-1504. https://doi.org/10.1126/science.1126215

[23] Zhang, Y., et al. (2014). Experimental and theoretical studies of serpentine microstructures bonded to prestrained elastomers for stretchable electronics. Advanced Functional Materials, 24(14), 2028-2037. https://doi.org/10.1002/adfm.201302949

[24] Wang, Y., et al. (2014). Wearable and highly sensitive graphene strain sensors for human motion monitoring. Advanced Functional Materials, 24(29), 4666-4670. https://doi.org/10.1002/adfm.201400379

[25] Bao, R., et al. (2018). Flexible and transparent triboelectric nanogenerators: Materials, devices, and applications. Advanced Materials, 30(21), 1804910. https://doi.org/10.1002/adma.201804910

[26] Yang, S., et al. (2023). Omnidirectional airflow sensors based on origami structure for flexible electronics. Advanced Intelligent Systems, 5(3), 2200209. https://doi.org/10.1002/aisy.202200209

[27] Che Abdullah, S., Dzulhelmy bin Amari, M., & Shafiq bin Abdullah Sabil, A. (2018). Simulation in single and multi-flow direction of airflow sensor. International Journal of Engineering and Technology, 7(4.27), 83–86.

[28] Yusoff, M. H., Che Abdullah, S., Mohamed Nasser, N. S., & Amari, M. D. (2023). Calibration method for flap structure of macrofluidic airflow sensor. AIP Conference Proceedings, 2571, 050001. https://doi.org/10.1063/5.0128419

[29] Dzulhelmy bin Amari, M., Saifuddin b. Abdull Shukor, M., & Che Abdullah, S. (2018). Optimization of velocity flap structures in high sensitivity macrofluidic airflow sensor. International Journal of Engineering & Technology, 7(4.27), 11–15.

[30] Che Abdullah, S., Dzulhelmy bin Amari, M., Mat Jusoh, M. A., & Aziz, F. A. (2020). Design optimization and experimental verification of air sensor's calibration tool. International Journal of Mechanical Engineering and Robotics Research, 9(4), 624–629.

[31] Dzulhelmy bin Amari, M. (2021). Data characterization and mapping validation of developed macrofluidic dynamic airflow sensor (Doctoral dissertation, Universiti Teknologi MARA).

[32] Amari, M. D. B., Che Abdullah, S., & Ahmad Kamil, M. I. H. B. (2019). Verification test of high flap macrofluidic air flow sensor in wind tunnel. International Journal of Engineering and Advanced Technology (IJEAT), 8(6), 1516–1519.

[33] Muhamad, W. A. N., Izzat, M., & Sakri, B. I. N. (2021). Calibration of new design flex sensor for airflow sensor.

[34] Saggio, G., et al. (2015). Resistive flex sensors: a survey. Smart Materials and Structures, 25(1), 013001. https://doi.org/10.1088/0964-1726/25/1/013001

[35] Hertzog, P. E., & Swart, A. J. (2015). A customizable energy monitoring system for renewable energy systems. In Proceedings of the 23rd Southern African Universities Power Engineering Conference, 154-159.

[36] Trung, T. Q., & Lee, N. E. (2016). Flexible and stretchable physical sensor integrated platforms for wearable human-activity monitoring and personal healthcare. Advanced Materials, 28(22), 4338-4372. https://doi.org/10.1002/adma.201504244